agriculture

Article

Design and Experimental Testing of an Overhead Rail Automatic Variable-Distance Targeted Spray System for Solar Greenhouses

Yahui Luo, Defan Huang, Ping Jiang, Siliang Xiang, Jianfei Liu, Minzi Xu and Yixin Shi *

College of Mechanical and Electrical Engineering, Hunan Agricultural University, Changsha 410128, China; luoyh@hunau.edu.cn (Y.L.); huangdefan@stu.hunau.edu.cn (D.H.); 1233032@hunau.edu.cn (P.J.); xiangsiliang@stu.hunau.edu.cn (S.X.); liujianfei@stu.hunau.edu.cn (J.L.); xmzzrn@stu.hunau.edu.cn (M.X.)
* Correspondence: shiyixin@hunau.edu.cn

Abstract: Crop cultivation in solar greenhouses is affected by issues such as low levels of automation in spraying machinery, inefficient spraying, and a lack of suitable spraying equipment for vertically cultivated crops, all of which are in urgent need of resolution. To address these problems, this paper proposes a suspended-rail automatic variable-distance targeted spray system. The rated working speed of the spray system is 0.3 m/s, and the rated working pressure is 0.3 MPa. This system achieves precise spraying of crops at varying heights by dynamically adjusting the position of the spray nozzle. To ensure accuracy in spraying, the system employs a laser ranging sensor for real-time measurement of crop positions and spraying distances. Combined with a parameter processing scheme, the system generates control signals to adjust the operation of the electric push rod and electromagnetic valve, thereby dynamically adjusting the spraying distance and timing. Using vertically cultivated potted peppers as experimental subjects, this study compares the performance of fixed- and variable-distance spraying modes. The results indicate that, compared to the fixed-distance mode, the automatic variable-distance mode increases pesticide adherence by 16.65% and reduces pesticide usage by 29.58%. The proposed suspended-rail automatic variable-distance targeted spray system offers an effective technical solution for the precise spraying of vertically cultivated crops in solar greenhouses and thus contributes to improved pesticide utilization efficiency, reduced pesticide residue, and lower environmental pollution.

Keywords: suspended-rail sprayer; targeted spraying; automatic variable distance; vertical cultivation

Citation: Luo, Y.; Huang, D.; Jiang, P.; Xiang, S.; Liu, J.; Xu, M.; Shi, Y. Design and Experimental Testing of an Overhead Rail Automatic Variable-Distance Targeted Spray System for Solar Greenhouses. *Agriculture* **2023**, *13*, 1853. https://doi.org/10.3390/agriculture13091853

Academic Editor: Giuseppe Manetto

Received: 4 September 2023
Revised: 17 September 2023
Accepted: 19 September 2023
Published: 21 September 2023

1. Introduction

Solar greenhouses maintain an environment of high temperature and humidity for prolonged periods of time during crop growth, resulting in a high incidence of pests and diseases [1]. In order to increase crop yields, high-frequency, large-dose pesticide spraying is widely used to control pests and diseases [2,3]. At present, the spraying machinery used in solar greenhouses in China is still dominated by backpack sprayers. As a result, applicators are exposed to a closed environment full of pesticides for lengthy periods, with consequent risks to health and safety [4–6]. For this reason, the development of pesticide spraying machinery suitable for China's solar greenhouses is a matter of high practical significance for improving pesticide utilization, protecting the health of pesticide applicators, and reducing environmental pollution [7–12].

In recent years, many researchers have conducted research on spray machinery for solar greenhouses, and a number of notable results have been achieved. For example, Alireza Rafiq et al. [13] designed an autonomous robot for greenhouse spraying that uses hot water pipes as guides, is controlled by AVR microcontrollers, and can cover most of the area that needs to be sprayed. I. N. Lee et al. [14] designed an accurate driving algorithm for greenhouse sprayers, which can automatically steer and track a guide rail in

complex road conditions and achieve an optimal turning radius. Luciano Cantelli et al. [15] developed a small multifunctional robot for autonomous spraying. This is equipped with an intelligent spraying system, which enables it to meet the spraying needs of different crops. Mohd Saiful Azimi Mahmud et al. [16] introduced a multi-objective algorithm for planning greenhouse pesticide spraying paths. This generates paths based on a virtual environment and on probabilistic road maps; these paths are then optimized with the NSGA-III algorithm. Dipak S. Khatawkar et al. [17] designed an electrostatic-induction spray-charging device for backpack sprayers and found that the charge-to-mass ratio was highest at 5 kV voltage, 5 mm away from the atomization zone. Zhang Yueshun [18] designed an inter-row sprayer for solar greenhouses, which includes an additional working mode for spray bar lifting and spray bar fixation, producing inter-row spray and ordinary spray, respectively. Yanjie Li et al. [19] compared a new air-assisted sprayer with two traditional sprayers with respect to spray deposition, loss and residue resulting from usage in the working environments of greenhouses and fields; their results proved the superiority of the new sprayer. Li Yang et al. [20] designed a new type of autonomous air-assisted sprayer and developed a corresponding spray optimization strategy so that droplets were uniformly deposited on the crop. Shi Shuo [21] designed a single-rail greenhouse sprayer and established a vibration model of the sprayer rail system; based on this, a vibration-damping design for the spray system was obtained. Ma Guoyi et al. [22] developed a self-propelled air sprayer suitable for greenhouses, which can adjust the height and angle of the fan according to the growth of the crop canopy to meet the needs of crop spraying at different growth stages. Xin Tonghui [23] designed a self-propelled electrostatic sprayer, which improves the applicable scenarios and spraying accuracy of the sprayer through coordinated control of the self-propelled module and the electrostatic spray module. Zhang Rensheng [24] designed a greenhouse target variable-spray device control system, which obtains target information through a laser rangefinder, controls the opening and closing of the solenoid valve and the electromagnetic proportional control valve, and enables variable spray targeting in greenhouses. Yang Zhenghe et al. [25] designed a greenhouse target spray robot, which detects crop information through LiDAR and controls the opening and closing of the solenoid valve on this basis to achieve target spraying. Finally, Zhang Yan [26] designed a solar greenhouse spraying system, which integrates the functions of wind transmission, static electricity, and high-pressure mist and realizes the functions of droplet air transmission, electrostatic adsorption, and overall indoor diffusion.

Each of the above-mentioned mechanical spray methods has its own advantages with respect to soil-cultivated greenhouse crops. However, researchers in this field have mainly focused on traditional greenhouse cultivation methods, and there has been relatively little research on the problems associated with spraying crops cultivated three-dimensionally in greenhouses. In this study, therefore, we sought to address the problems associated with spraying vertically cultivated crops by designing a hanging-rail-type automatic variable-pitch target spray system with the characteristics of real-time adjustable spray distance. This enables automatic adjustment of the position of the spray head according to the position of the crop and the shape of the crop canopy so that the best spray distance is maintained and spray uniformity is effectively improved. In pursuit of our study aims, we carried out a series of spray-deposition tests to analyze the application of the hanging-rail automatic variable-pitch target spray system in a plant protection operation involving three-dimensionally cultivated crops in a solar greenhouse. In the course of these tests, the applicability, efficacy and performance of the system were comprehensively evaluated in order to provide a reference for the design and performance optimization of spray mechanisms for three-dimensionally cultivated crops in solar greenhouses.

2. Materials and Methods

2.1. Overall Structure and Working Principle

Figure 1 shows the structure of the hanging-rail automatic variable-pitch directional spray system for solar greenhouses designed for this study. The key components of

the system include a mounting frame, self-propelled system, control system, guide rail, spraying arm, power supply system, drug supply system, and remote-control device. The main technical parameters of the spray system are listed in Table 1.

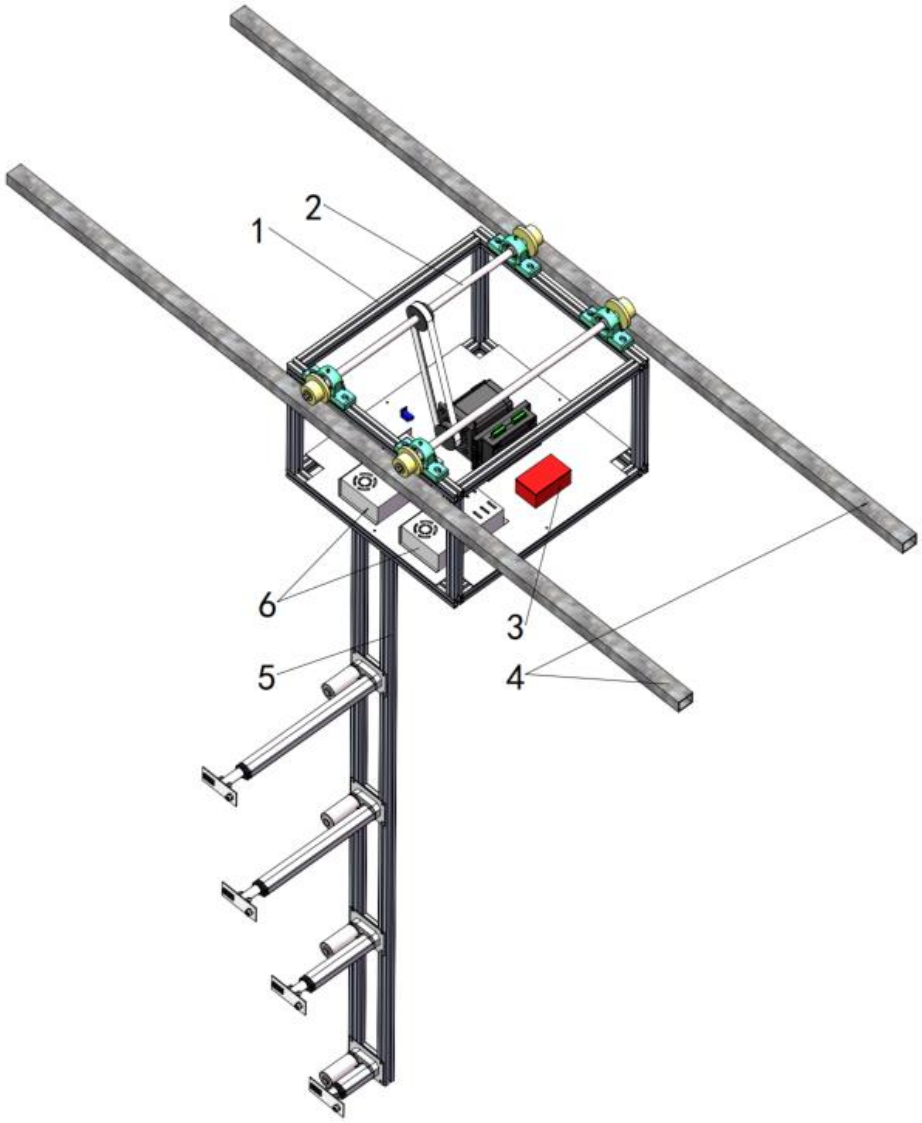

Figure 1. Schematic diagram of the spraying machine. 1. Mounting frame; 2. Self-propelled system; 3. Control box; 4. Guide rail; 5. Spraying arm; 6. Power supply system.

Table 1. Main technical parameters of the overhead-rail automatic variable-range targeted spraying system.

Item	Numerical
Dimensions of the spraying system (length × width × height)/mm	500 × 60 × 2000
Spraying system quality/kg	50
Rated operating pressure/MPa	0.3
Maximum working pressure/MPa	0.5
Number of nozzles/pieces	4
Nozzle type	Fan-shaped nozzle
Spray angle/degrees	60
Rated operating speed/(m/s)	0.3
Maximum operating speed/(m/s)	0.5

The working principle of the system may be briefly stated. After the system is started with the remote-control device, the spray host moves forward along the guide rail under the drive of the self-propelled system, and the drug supply system begins to deliver the liquid to the spray system. Each laser ranging sensor continuously detects the distance at each height and sends these data to the single-chip microcomputer in real time. The single-chip microcomputer compares the received data with the set distance range to determine whether the current distance is within the set range. If the current distance meets the requirements, the microcomputer calculates the difference between the current distance and the target distance and then gives output control instructions, allowing the corresponding electric actuator to move and open the corresponding solenoid valve to achieve precise target spray. Figure 2 presents the working principle of the system in schematic form. Figure 3 presents the spray configuration of the system in schematic form.

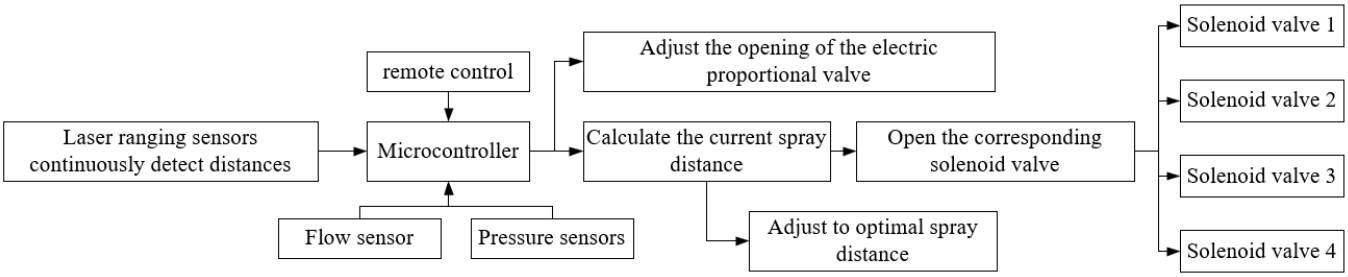

Figure 2. Schematic diagram of the working principle of the system.

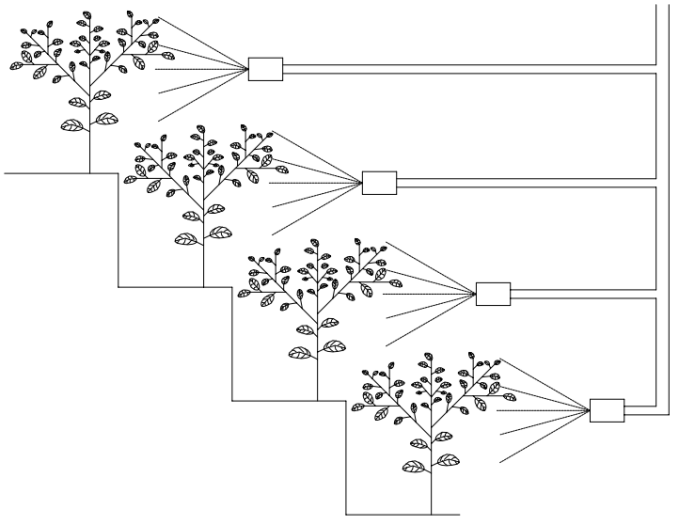

Figure 3. Schematic diagram of the spray configuration.

2.2. Design of Key Components

2.2.1. Design of Spraying Arm Structure

Crop plants in vertical cultivation are distributed across multiple layers so that individual plants are situated at different heights and horizontal positions. To ensure that every layer of crops receives comprehensive and uniform spray coverage, an efficient spraying arm structure was designed for this study. The spraying arm primarily consists of the spraying arm itself, as well as a mounting plate, laser distance sensor, nozzles, electromagnetic valves and other components. The structure of the spraying arm is illustrated in Figure 4.

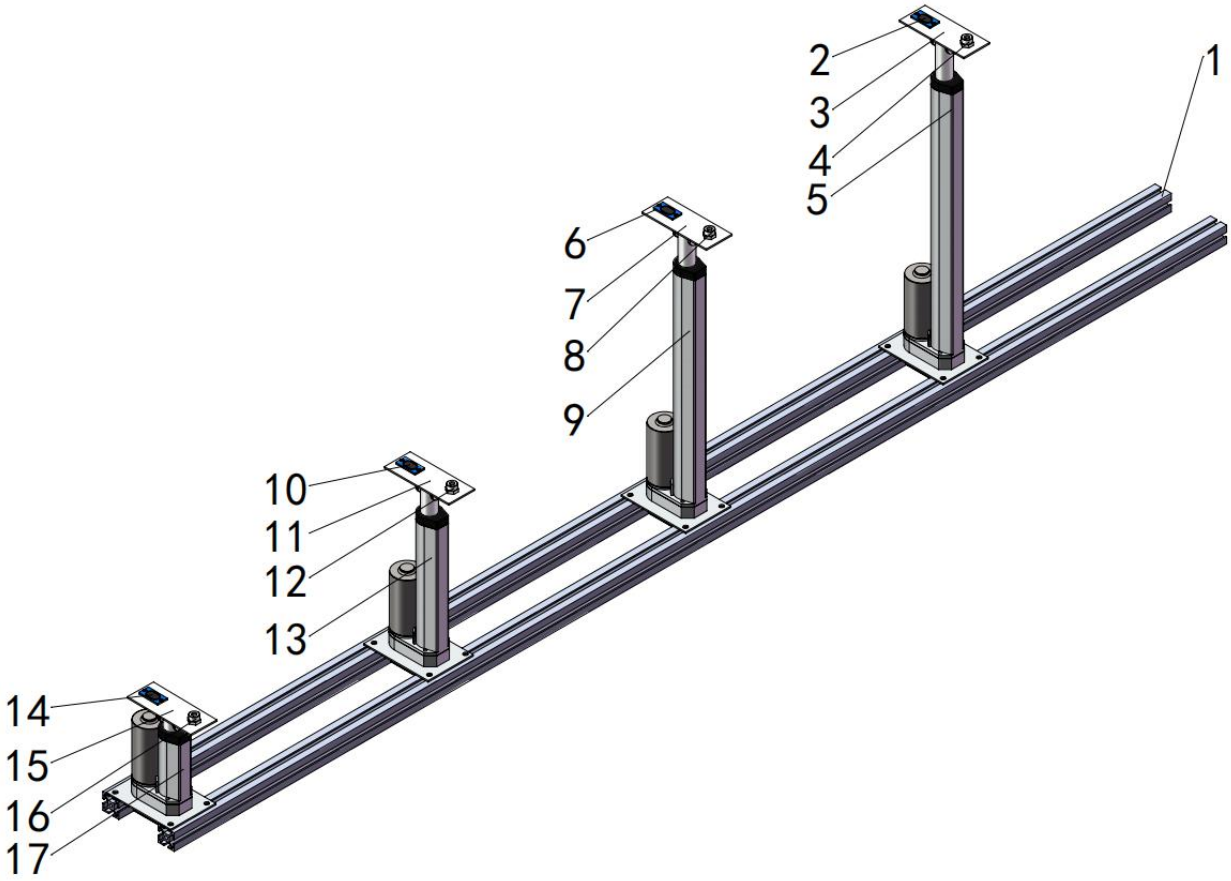

Figure 4. Schematic diagram of the spraying arm structure. 1. Spraying gantry; 2, 6, 10, 14. Laser distance sensors; 3, 7, 11, 15. Mounting plates; 4, 8, 12, 16. Fan-shaped nozzles; 5. First electric actuator; 9. Second electric actuator; 13. Third electric actuator; 17. Fourth electric actuator.

The spraying arm consists of four parts, corresponding to the top layer, middle and upper layer, middle and lower layer, and bottom layer of the three-dimensional cultivation rack. Each section is equipped with a sector nozzle, a laser ranging sensor, and an electric actuator with different strokes. The fan-shaped nozzle can produce uniform and fine droplets so that the chemical solution is evenly attached to the surface of the crop. The laser ranging sensor can detect the position of the plant and the distance between the nozzle and the plant in real time and can transmit the detected data to the single-chip microcomputer. The electric actuator can adjust the distance between the nozzle and the canopy according to the control signal output produced by the microcomputer so as to achieve precise spraying of plants at different levels. The laser ranging sensor and the sector nozzle are mounted at the same horizontal height on a mounting plate, and the horizontal distance between the two is determined by the forward speed of the spray system, the response time of the solenoid valve, and the response time of the control system; The electric actuator is mounted on the back of the mounting plate, and the installation height is determined by the height difference between the adjacent two floors of the three-dimensional cultivation rack and the height of the crop.

2.2.2. Design of Autonomous Movement System

In order to make the spray host move smoothly along the guide rail, we designed a self-propelled system. This consists of a self-propelled motor, active shaft, driven shaft, active pulley, driven pulley, belt, T-wheel, bearing seat and other parts; its structure is shown in Figure 5.

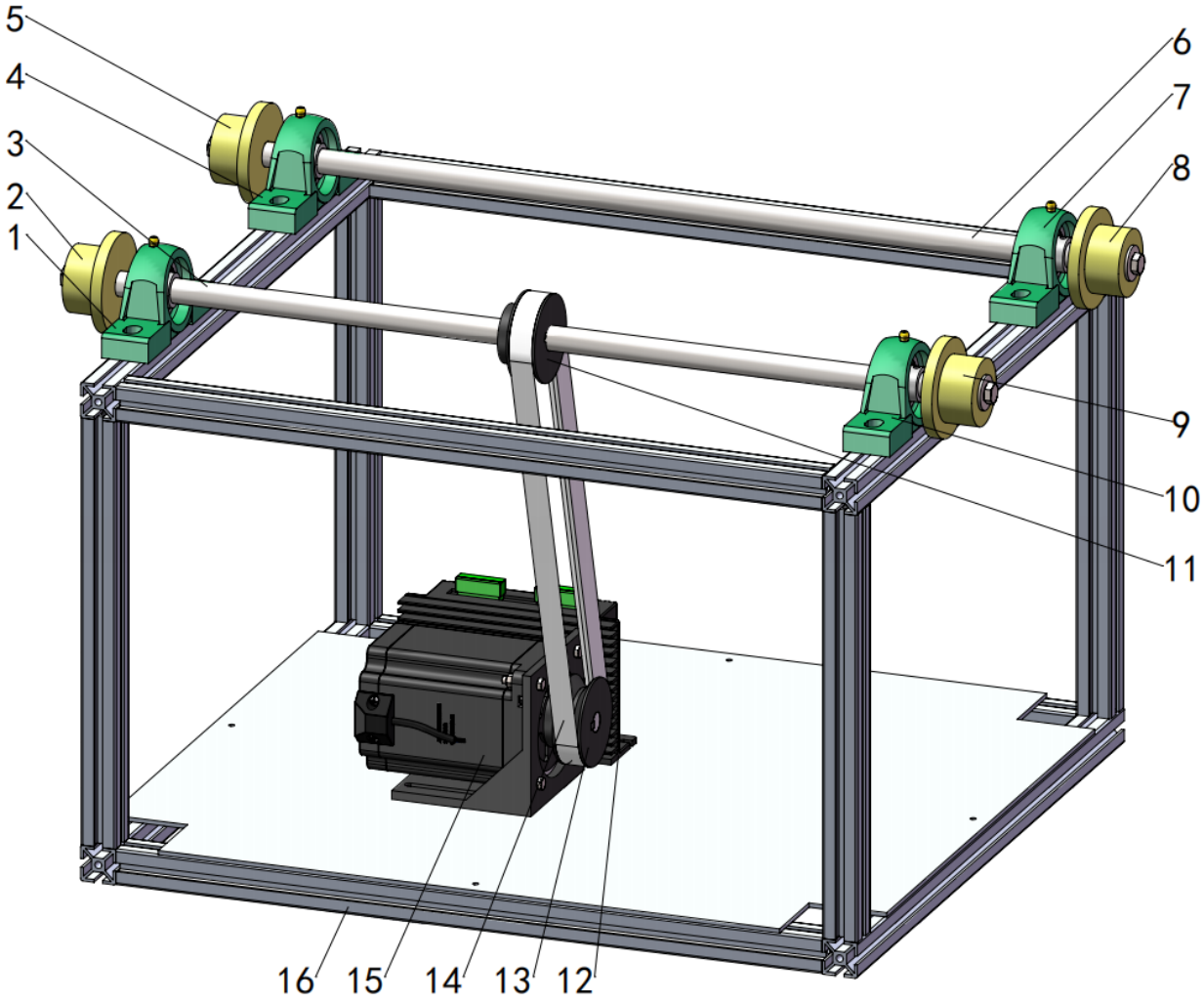

Figure 5. Schematic diagram of the self-propelled system. 1, 4, 7, 10. Bearing seat; 2, 5, 8, 9. T-type wheel; 3. Drive shaft; 6. Driven shaft; 11. Driven pulley; 12. M860 driver; 13. Active pulley; 14. A-type belt; 15. Self-propelled motor; 16. Mounting bracket.

During operation, the stepper motor acts as a power source, and the key parameters of its output power, such as speed, direction and torque, are precisely controlled by the stepper motor driver. This enables the stepper motor to flexibly adjust its speed and direction according to different operating speed and direction requirements. At the same time, it can also flexibly output torque according to the load, speed and working environment of the system; this ensures that the stepper motor does not lose step and overload during the working process. The power output by the stepper motor is transmitted to the active shaft through the transmission device composed of the active pulley, belt and driven pulley; this drives the active shaft to rotate, which then drives the T-wheel to rotate so that smooth movement of the spray host is achieved.

2.2.3. Structural Design of Drug Supply System

The drug supply system is shown in Figure 6. This is composed of key parts, which include a medicine box, filter, electric diaphragm pump, pressure sensor, flow sensor, electric proportional valve and solenoid valve.

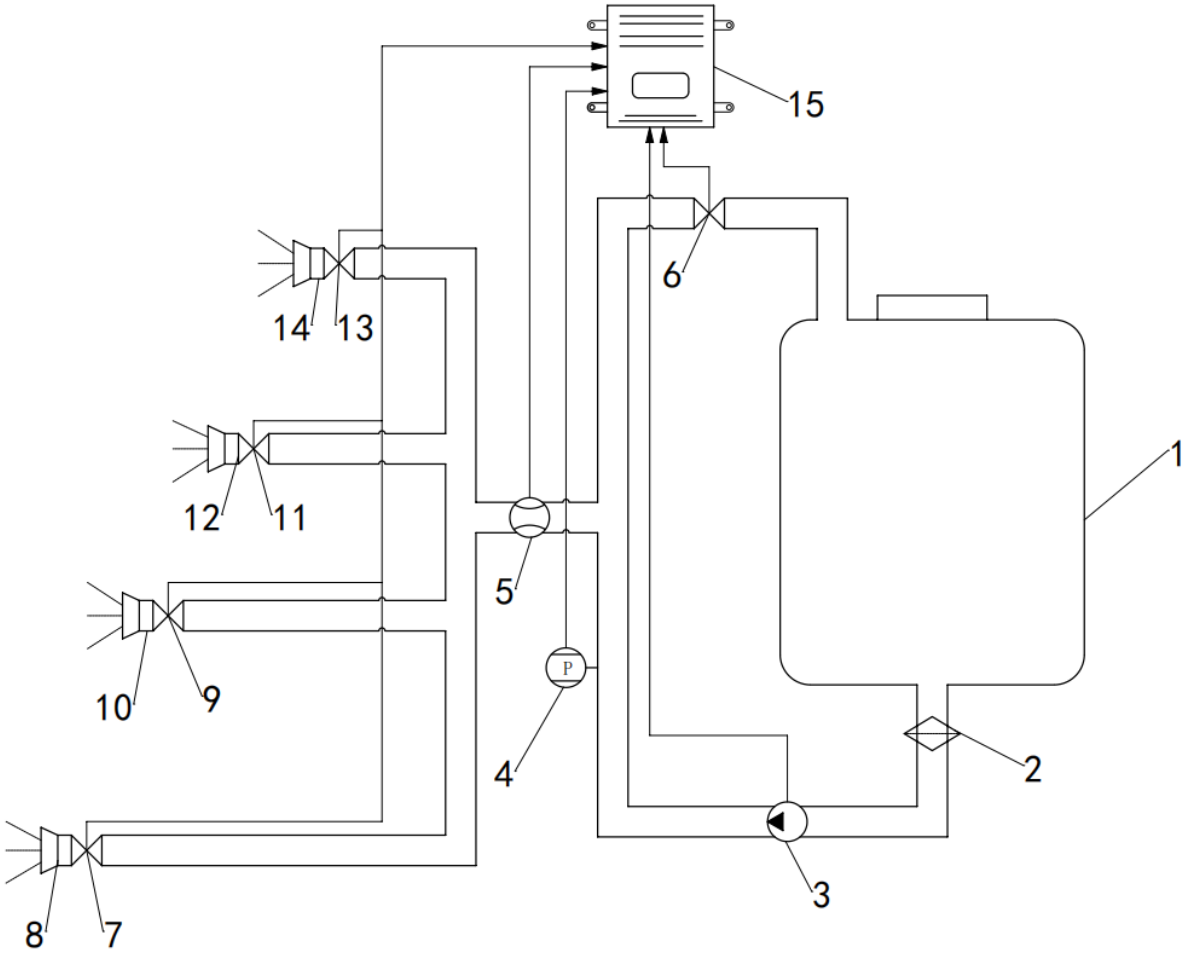

Figure 6. Schematic diagram of the medication system. 1. Water tank; 2. Filter; 3. Electric diaphragm pump; 4. Pressure sensor; 5. Flow sensor; 6. Electric proportional valve; 7, 9, 11, 13. Solenoid valve; 8, 10, 12, 14. Nozzle; 15. Control box.

During operation, the electric diaphragm pump extracts the liquid filtered by the filter from the medicine tank and pumps it into the supply line. The pressure sensor and flow sensor continuously monitor the pressure and flow of the chemical liquid in the drug supply pipeline and transmit the real-time data to the single-chip microcomputer, which calculates the opening degree of the electric proportional valve according to the received data and outputs the corresponding control instructions to control the electric proportional valve to ensure that the pressure and flow of the chemical liquid in the drug supply pipeline are always stable within the preset range. The system also includes automatic alarm and protection functions. When there is insufficient liquid in the drug supply system, or when there is a blockage, leak or any other fault which leads to abnormal liquid pressure, the single-chip microcomputer outputs a corresponding control signal so that the electric diaphragm pump stops working, and beeps an alarm sound, prompting the operator to carry out necessary inspection and maintenance. By such means, the safety and reliability of the system is ensured.

2.2.4. Composition of Control System

The control system is mainly composed of a single-chip microcomputer, relay, electric diaphragm pump, electric proportional valve, stepper motor driver, laser ranging sensor, photoelectric switch, solenoid valve and DC motor forward/reverse drive module, as well as other parts, as shown in Figure 7.

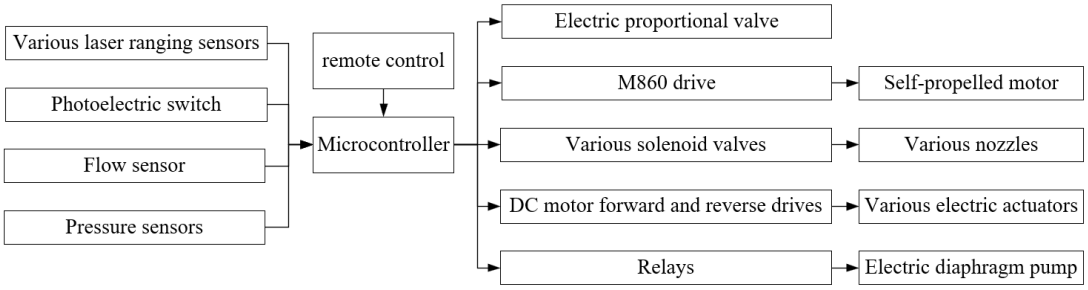

Figure 7. Components of the control system.

Among these components, the single-chip microcomputer is an STM32F103ZET6-type single-chip device produced by ST, which integrates a high-performance ARM Cortex-M332-bit RISC core and high-speed embedded memory, is rich in interface resources and peripheral devices, and can adapt to the high temperature and high humidity operating environment of a greenhouse; in short, it is well suited to the design requirements of the present study. The relay is used to control the start and stop of the electric diaphragm pump, which can be controlled by the switching signal issued by the single-chip microcomputer. The electric proportional valve is used to adjust the actual pressure of the chemical solution; its opening and closing can be controlled by the signal output by the single-chip microcomputer so that accurate control of the chemical solution may be achieved. The stepper motor driver adopts an MA860-type driver, which connects the single-chip microcomputer, power supply and stepper motor through the stepper motor driver so that precise control of the stepper motor by the single-chip microcomputer may be achieved. The laser ranging sensor has a detection distance range of 4–400 cm and is used to detect the target position and spray distance, and then sends these data to the single-chip microcomputer. The photoelectric switch detects obstacles in a range of 1–30 cm and always remains closed during normal operation; however, when obstacles are detected, the photoelectric switch sends a signal to the single-chip microcomputer. The solenoid valve is used to control the start and stop of the spray, and each solenoid valve is controlled by the multi-channel switching signal output by the single-chip microcomputer. The DC motor forward/reverse drive is used to control the telescopic operation of the electric actuator, and each driver is controlled by the multiple pulse signals output by the single-chip microcomputer.

2.3. Spray Parameter Adjustment Scheme and Control System Design

2.3.1. Spray Distance Adjustment Scheme

The selected nozzle is a conventional fan-shaped nozzle (manufactured by Dongguan Yusheng Spray Purification Co., Ltd., Dongguan, China) with a spray angle of 60° and a flow rate of 0.39 L/min. The relationship between spray distance and coverage area is illustrated in Figure 8 (the dashed line in the figure represents the angle bisector).

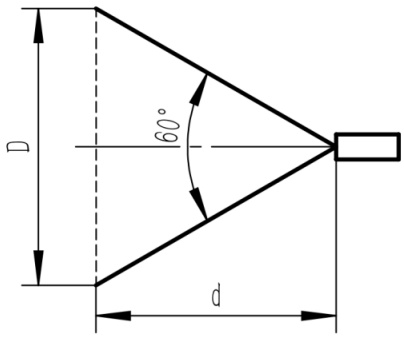

Figure 8. Spray distance and coverage area.

As can be seen from Figure 8, the relationship between spray distance and spray coverage may be expressed as thus:

$$D = 2d \times \tan 30^{\circ} \quad (1)$$

In the above equation:
D is Vertical coverage range of spray, in cm; and
d is Spray distance, in cm.

From field measurements, it may be determined that the average height of peppers in the flowering and fruit setting stage is about 30 cm. In order to ensure the best spray effect, the spray distance must be adjusted to the optimal spray distance d_f. Given a D value of 30 cm, to ensure that the droplets fully cover the pepper canopy, we may use Equation (1) to calculate an optimal spray distance d_f of about 26 cm.

When the laser ranging sensor of the spraying system detects the pepper plant, because the spray head and the laser sensor are in the same plane, the distance measured by the sensor at this time can be approximated as the spray distance and may be expressed as thus:

$$d_0 \approx d_1 \quad (2)$$

In the above equation:
d_0 is distance from the nozzle to the plants, in cm; and
d_1 is the distance between the laser distance sensor and the plants, in cm.

The measured spray distance d_0 is compared with the optimal spray distance d_f and automatically adjusted; if $d_0 > d_f$, the electric actuator moves forward close to the canopy, and vice versa, moves away from the canopy. The distance traveled by the electric actuator may be expressed as thus:

$$d_t = \left| d_0 - d_f \right| \quad (3)$$

In the above equation:
d_t is distance of electric actuator movement, in cm.

The movement time of the electric actuator may be expressed thus:

$$t = \frac{10 d_t}{v} \quad (4)$$

In the above equation:
t is the movement time of the electric actuator, in seconds; and
v is the movement speed of the electric actuator, set at 20 mm/s.

2.3.2. Automatic Variable-Range Target Spray Control Flow

The automatic variable-pitch target spray control system can automatically adjust the distance between the spray head and the plant, as well as the opening and closing of the solenoid valve according to the position, height and shape of the plant, so as to improve the spray efficiency and accuracy.

The control process may be briefly stated. After powering on, the operator activates the entire system via the remote control and waits for the system to finish initializing. After the system initialization is completed, the spray host advances along the guide rail at a speed of 0.3 m/s. At the same time, the single-chip microcomputer sends instructions to the electric diaphragm pump to start the drug supply system and provides the liquid to the spray device. Each laser ranging sensor continuously detects the distance and transmits the measurement results to the microcontroller in real time.

The microcontroller compares the received signal with the optimal spray distance and calculates the difference between the two and the time required for the movement of the electric actuator. If the difference is positive, the microcontroller instructs the electric actuator to extend or retract so that an optimal spray distance between the nozzle and the target is maintained. At the same time, the microcontroller instructs the corresponding

solenoid valve to open, and the chemical liquid is sprayed from the nozzle to achieve effective spraying of the target area.

Once the distance detected by the laser ranging sensor exceeds the set range, the single-chip microcomputer quickly instructs the solenoid valve to close; spraying is thus paused, ensuring that the chemical solution is not sprayed by mistake. The system then repeats the control process until the distance detected by the laser ranging sensor is back within the set range.

When the single-chip microcomputer receives the data sent by the photoelectric switch, the system turns off all solenoid valves and laser ranging sensors in turn and stops the forward movement until the next instruction is issued. If the photoelectric switch stops sending signals to the single-chip microcomputer within 5 s, the single-chip microcomputer sends a control signal to the stepper motor controller; this drives the spray host to continue to move and work according to the above workflow. If the photoelectric switch continues to send signals to the microcomputer after 5 s, the microcomputer instructs the spray device to return to the initial position at the maximum working speed, thereby ending the spray process. The control process is shown in flowchart form in Figure 9.

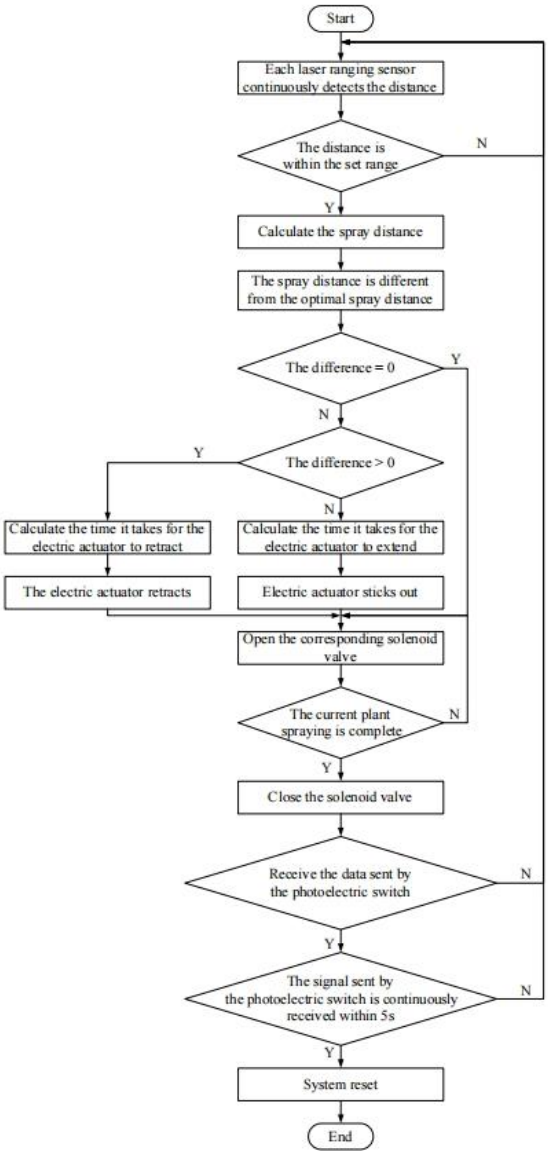

Figure 9. Control flowchart.

2.4. Test Conditions

In order to verify the spraying effect of the hanging-rail-type automatic variable pitch on the target spray system in practical applications, systematic spraying was carried out in a solar greenhouse. The test site selected was the solar greenhouse on the roof of the eighth teaching building of Hunan Agricultural University, and the test date was 10 April 2023. In the experiment, 12 pots of potted peppers were selected as test subjects. Each pot of peppers was numbered and placed on a three-dimensional cultivation rack in a specific order, as shown in the photograph in Figure 10.

Figure 10. Numbering and placement of pepper plants.

Before the test, refer to the standard JB/T 9782-2014 [27], paper clips were used to evenly fix water-sensitive test strips on the top, middle and lower positions of the pepper canopy. At the same time, the layout position of each water-sensitive test strip was recorded to ensure that the arrangement positions of the strips were the same in different groups of tests so as to improve the accuracy and comparability of the test results. In addition, before each trial, the initial volume of the liquid in the medicine box was recorded.

For the purposes of our study, two groups of spray tests were designed. The first group was a fixed-distance target spray test. In this group of experiments, the target spray system worked continuously, while the spray distance adjustment system did not work, ensuring that the spray distance remained constant. In this mode, when the position detected by a

laser ranging sensor was within the set range, the microcontroller instructed the solenoid valve to open and start continuous spraying. The second group was an automatic variable-pitch target spray test, in which the target spray system and the spray distance adjustment system operated simultaneously. When the position detected by a laser ranging sensor was within the set range, the single-chip microcomputer automatically calculated the moving distance and direction of the electric actuator and controlled the corresponding electric actuator movement. At the same time, the corresponding solenoid valve was opened and spraying continued until all the peppers were sprayed.

To improve the reliability of the test data, four independent replicates were performed for each set of spray tests. During spraying, all tests maintained a forward speed of 0.3 m/s. After each spray, the water-sensitive test strips from different canopy areas were collected, air-dried, and carefully stored in pre-numbered dry test bags to ensure the integrity and reliability of the experimental data. At the same time, the volume of the liquid remaining after the test was recorded. The test arrangement is shown in Figure 11, and the spray effect is shown in Figure 12.

Figure 11. Test setup.

Figure 12. Spray effect.

3. Test Results and Analysis

After two sets of spray tests according to the above experimental methods, the water-sensitive test strips stored in the test bag were analyzed according to different areas and then given one of the following five grades: invalid grade 0 (no chemical solution adhesion); effective grade 1 (the adhesion area of the chemical solution accounted for 0–1/4 of the water-sensitive test strip); effective grade 2 (the adhesion area of the chemical solution

accounted for 1/4–1/2 of the water-sensitive test strip); effective grade 3 (the adhesion area of the chemical solution accounted for 1/2–3/4 of the water-sensitive test strip); or effective grade 4 (the adhesion area of the chemical solution accounted for 3/4 of the water-sensitive test strip). Direct grading was carried out for water-sensitive test strips that could be judged by the naked eye; for strips that could not be judged by the naked eye, ImageJ software was used to calculate and grade the adhesion area (the dark area on the water-sensitive test strip). The water-sensitive strip adhesion area analysis is shown in Figure 13.

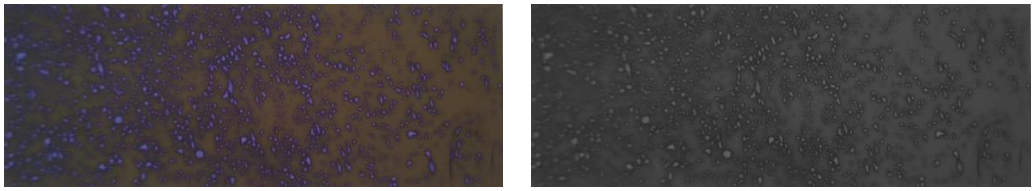

(**a**) (**b**)

Figure 13. Spray adhesion-area analysis. (**a**) Original image. (**b**) Grayscale chart.

After grading all of the water-sensitive test strips, the adhesion rate of the drug solution in different regions of the two sets of experiments was calculated according to Equation (5). The adhesion rate of the drug solution to the target spray at fixed distances is shown in Figure 14, and the adhesion rate of the drug solution to the target spray at automatic variable distances is shown in Figure 15.

$$\text{Liquid deposition volume} = \frac{N_1 \times 1 + N_2 \times 2 + N_3 \times 3 + N_4 \times 4}{N \times 4} \times 100\% \quad (5)$$

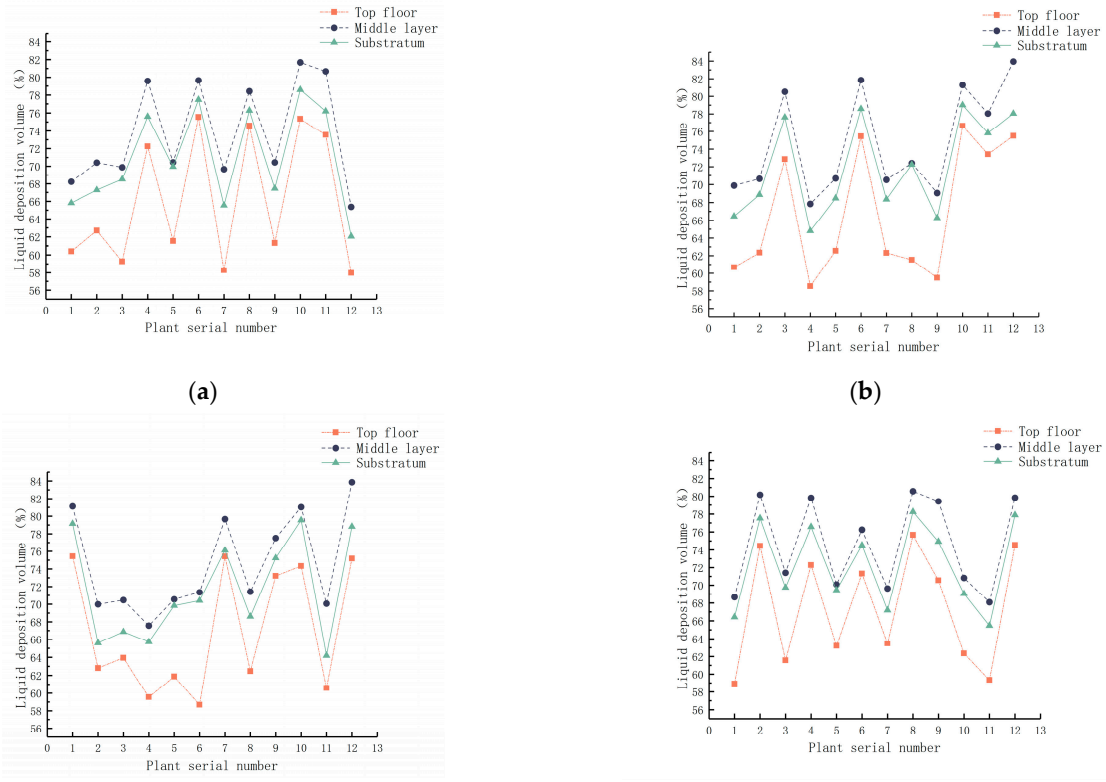

(**a**) (**b**)

(**c**) (**d**)

Figure 14. Fixed-distance adhesion rate of target spray solution. (**a**) Fixed-distance target spray group 1. (**b**) Fixed-distance target spray group 2. (**c**) Fixed-distance target spray group 3. (**d**) Fixed-distance target spray group 4.

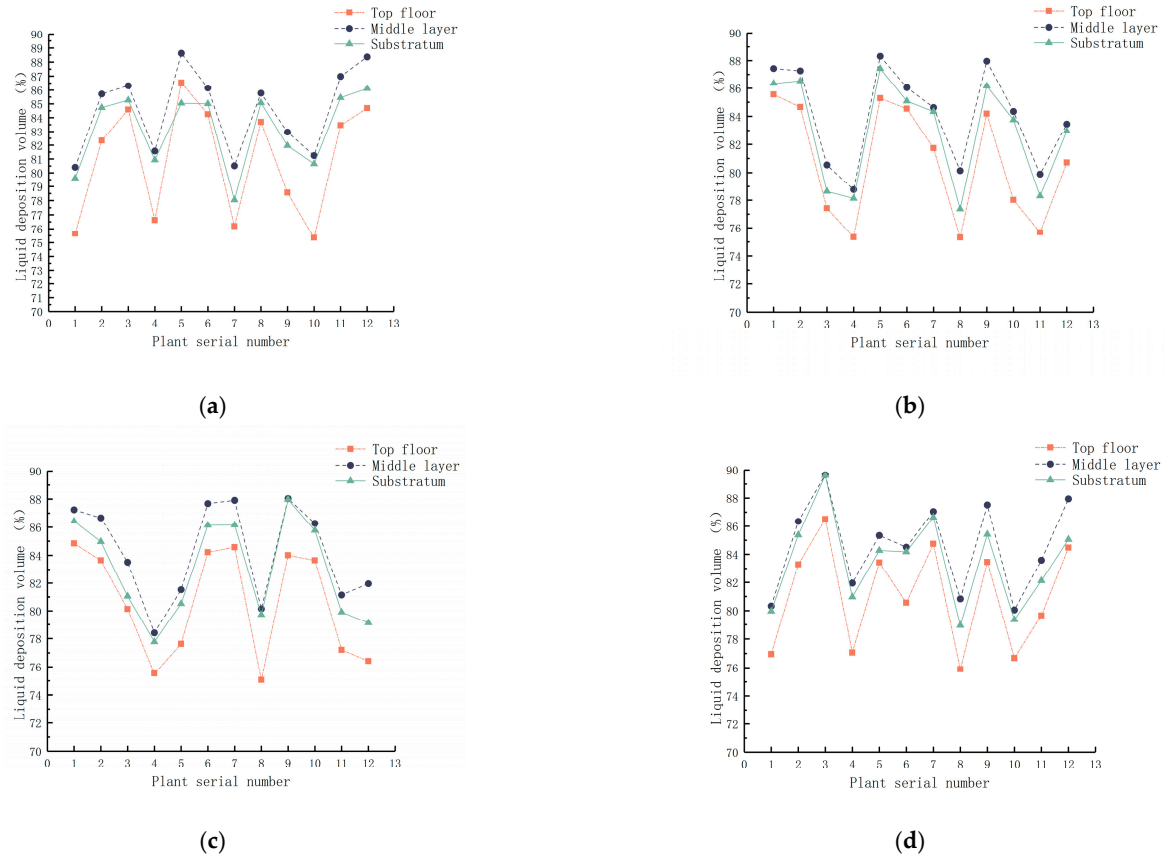

Figure 15. Automatic variable-pitch adhesion to target spray solution. (**a**) Automatic variable-pitch target spray group 1. (**b**) Automatic variable-pitch target spray group 2. (**c**) Automatic variable-pitch target spray group 3. (**d**) Automatic variable-pitch target spray group 4.

In the above equation:
N_1 is the number of effective stage 1 blades;
N_2 is the number of effective stage 2 blades;
N_3 is the number of effective stage 3 blades;
N_4 is the number of effective stage 4 blades; and
N is the total number of observed blades.

In order to investigate differences in droplet attachment rate in different spray modes, the calculated data were further analyzed. For each mode, the mean, standard deviation and coefficient of droplet adhesion rate were calculated, and the results are presented in Table 2.

Table 2. Droplet adhesion analysis table by mode.

Spray Mode	Canopy Position	Average/%	Standard Deviation	Coefficient/%
Fixed-pitch target spray	Top floor	66.78	6.80	10.19
	Middle layer	74.39	5.46	7.34
	Substratum	71.72	5.28	7.36
	Overall	70.96	6.65	9.37
Automatic variable-pitch target spray	Top floor	80.83	3.88	4.80
	Middle layer	84.36	3.21	3.81
	Substratum	83.13	3.26	3.92
	Overall	82.77	3.74	4.52

Looking at the data in Table 2, it can be seen that the automatic variable-pitch target spray produced better results than the fixed-distance target spray. Specifically, for the top, middle, lower and overall aspects, compared with the fixed-distance target spray, the average adhesion rates of the automatic variable-pitch target spray were 21.05%, 13.41%, 15.92% and 16.65% higher, the standard deviations were 43.00%, 41.19%, 38.26% and 43.76% lower, and the coefficients of variation were 52.91%, 48.14%, 46.73% and 51.78% lower, respectively. This series of data clearly proves that the automatic variable-pitch target spray not only significantly improves the adhesion rate of different parts but is also more stable and reliable in terms of adhesion rate fluctuations.

The initial and remaining doses of the two spray modes were calculated by analyzing the initial and remaining doses for each trial, as shown in Figure 16.

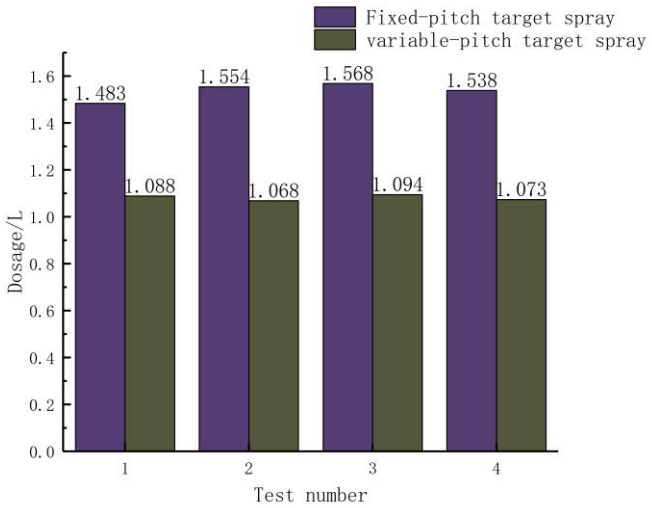

Figure 16. Medication dosage histogram.

According to the data presented in Figure 16, the average dosage of the automatic variable-pitch target spray was 29.58% lower than that of the traditional fixed-pitch target spray. This result proves that the automatic variable-pitch target spray system can not only improve the adhesion rate of the chemical solution but also effectively reduce the dosage.

4. Conclusions and Discussions

4.1. Conclusions

(1) The hanging-rail automatic variable-pitch target spray system described in this paper can meet the spraying requirements of three-dimensionally cultivated crops. In the spraying process, the single-chip microcomputer controls the movement of the electric pusher so that the distance between the nozzle and the target is always kept at the optimal spray distance; this ensures that the droplets fully and evenly cover the plant canopy, thereby improving their adhesion rate.

(2) Two groups of spray tests were carried out: an automatic variable-pitch target spray test and a fixed-distance target spray test. The spray adhesion rate was determined and analyzed using water-sensitive test strips and ImageJ1 software. The experimental results showed that when compared with fixed-distance target spray, automatic variable-pitch target spray increased the spray adhesion rate by 16.65% and reduced pesticide usage by 29.58%. These results prove that the hanging-rail automatic variable-distance target spray system described in this paper can improve the adhesion rate of chemical solution and reduce the amount of pesticide used.

4.2. Discussions

(1) The automatic variable distance target spray system designed in this paper controls the solenoid valve and electric actuator, respectively, according to the data of the laser

ranging sensor, so that the spray head keeps a set distance from each layer of crops. The droplet adhesion rate was increased by 16.65%. However, in the later stages of plant growth, the canopy spacing is too small to be needed and not suitable for spraying with this system. The system is only suitable for crops with small canopies and large plant spacing.

(2) This paper only used conventional sector nozzles for spray testing and did not make comparisons with other types of nozzles. In order to further improve the spray adhesion rate, subsequent studies can try other types of nozzles, such as "low thrust" nozzles or "bubble" nozzles, for comparative testing and then select the most suitable nozzle type.

(3) This paper only tests commonly used forward speed and spray pressure, and it is uncertain whether this combination of parameters is the best combination. Follow-up research can use orthogonal testing to find the best combination of the two to further improve the spray effect.

Author Contributions: Conceptualization, Y.L., P.J., Y.S. and D.H.; methodology, Y.L.; software, D.H.; site construction, D.H., J.L. and S.X.; data curation, Y.L. and D.H.; resources, M.X., J.L. and D.H.; writing, original draft preparation, D.H.; writing, review and editing, Y.L., D.H., Y.S. and P.J.; visualization, Y.L. and D.H.; supervision, Y.L., Y.S. and P.J.; project administration, Y.S.; funding acquisition, Y.L., Y.S. and P.J. All authors have read and agreed to the published version of the manuscript.

Funding: This work was supported by the Scientific Research Project of the Hunan Provincial Education Department (grant number 21B0203), the Changsha City Natural Science Foundation (grant number kq2208069), the Key R&D project of Hunan Province (grant number 2023NK2010), and a sub-project of the National Key R&D Plan (grant number 2022YFD2002001).

Conflicts of Interest: The authors declare no conflict of interest.

References

1. Xu, D.; Yang, X.; Li, X. Study on the occurrence and control of pests and diseases in solar greenhouse. *Agric. Sci. Technol. Equip.* **2021**, *442*, 20–21.
2. Sun, J.; Gao, H.; Tian, J.; Wang, J.; Du, C.; Guo, S. Development status and trend of facility horticulture in China. *J. Nanjing Agric. Univ.* **2019**, *42*, 594–604.
3. He, X. Technical equipment for precision pesticide application for plant protection. *Agric. Eng. Technol.* **2017**, *37*, 22–26.
4. Dhananjayan, V.; Ravichandran, B. Occupational health risk of farmers exposed to pesticides in agricultural activities. *Curr. Opin. Environ. Sci. Health* **2018**, *4*, 31–37. [CrossRef]
5. Li, C.; Zhao, L.; Xiong, B.; Zhang, L.; Li, Z.; Teng, F. Comparison of the application effect of four commonly used sprayers on plastic greenhouse tomato crops. *North. Hortic.* **2018**, *21*, 90–98.
6. Zheng, Y.; Chen, B.; Lv, H.; Kang, F.; Jiang, S. Research Progress of Mechanization Technology and Equipment for Orchard Plant Protection in China. *Trans. Chin. Soc. Agric. Eng.* **2020**, *36*, 110–124.
7. Grella, M.; Gallart, M.; Marucco, P.; Balsari, P.; Gil, E. Ground Deposition and Airborne Spray Drift Assessment in Vineyard and Orchard: The Influence of Environmental Variables and Sprayer Settings. *Sustainability* **2017**, *9*, 728. [CrossRef]
8. He, X. Research status and development suggestions of precision drug application technology and equipment in China. *Smart Agric.* **2020**, *2*, 133–146.
9. Hu, P.; Zhang, R.; Yang, J.; Chen, L. The development of domestic and foreign plant protection machinery and the prospect of intelligent integrated pest management system. *China Plant Prot. Guide* **2022**, *42*, 20–28.
10. Chen, H.; Lan, Y.; Fritz, B.K.; Hoffmann, W.C.; Liu, S. Research progress on the control of rice diseases and pests by plant protection UAV. *Jiangsu Agric. Sci.* **2023**, *51*, 38–49.
11. He, Y.; Wu, J.; Fang, H.; Zheng, Q.; Xiao, S.; Cen, H. Review on droplet deposition effect of plant protection UAV. *J. Zhejiang Univ. Agric. Life Sci.* **2018**, *44*, 392–398.
12. Lan, Y.; Yan, Y.; Wang, B.; Song, C.; Wang, G. Research status and development trend of key technologies of intelligent drug application robot. *Trans. Chin. Soc. Agric. Eng.* **2022**, *38*, 30–40.
13. Rafiq, A.; Kalantari, D.; Mashhadimeyghani, H. Construction and development of an automatic sprayer for greenhouse. *Agric. Eng. Int. CIGR e-J.* **2014**, *16*, 36–40.
14. Lee, I.; Lee, K.; Lee, J.; You, K. Autonomous Greenhouse Sprayer Navigation Using Automatic Tracking Algorithm. *Appl. Eng. Agric.* **2015**, *31*, 17–21.
15. Cantelli, L.; Bonaccorso, F.; Longo, D.; Melita, C.D.; Schillaci, G.; Muscato, G. A Small Versatile Electrical Robot for Autonomous Spraying in Agriculture. *AgriEngineering* **2019**, *1*, 391–402. [CrossRef]

16. Mahmud, M.S.A.; Abidin, M.S.Z.; Mohamed, Z.; Rahman, M.K.I.A.; Iida, M. Multi-objective path planner for an agricultural mobile robot in a virtual greenhouse environment. *Comput. Electron. Agric.* **2019**, *157*, 488–499. [CrossRef]
17. Khatawkar, D.S.; Dhalin, D.; James, P.S.; Subhagan, S.R. Electrostatic Induction Spray-charging System (Embedded Electrode) for Knapsack Mist-blower. *Curr. J. Appl. Sci. Technol.* **2020**, *39*, 80–91. [CrossRef]
18. Zhang, Y. Development and Experimental Study of Interrow Sprayer in Solar Greenhouse. Ph.D. Thesis, Shandong Agricultural University, Taian, China, 2019.
19. Li, Y.; Li, Y.; Pan, X.; Li, Q.X.; Chen, R.; Li, X.; Pan, C.; Song, J. Comparison of a new air-assisted sprayer and two conventional sprayers in terms of deposition, loss to the soil and residue of azoxystrobin and tebuconazole applied to sunlit greenhouse tomato and field cucumber. *Pest Manag. Sci.* **2018**, *74*, 448–455. [CrossRef]
20. Li, Y.; Yuan, J.; Liu, X.; Niu, Z.; Chen, B.; Liu, X. Spraying strategy optimization with genetic algorithm for autonomous air-assisted sprayer in Chinese heliogreenhouses. *Comput. Electron. Agric.* **2019**, *156*, 84–95. [CrossRef]
21. Shi, S. Design and Experimental Study of Single-Hanging Rail Greenhouse Sprayer. Master's Thesis, Jiangsu University, Zhenjiang, China, 2019.
22. Tian, F.; Xia, K.; Wang, J.; Song, Z.; Yan, Y.; Li, F.; Wang, F. Design and test of greenhouse self-propelled air-fed sprayer. *Chin. J. Agric. Mech.* **2020**, *41*, 54–61.
23. Xin, T. Development and Test of Electrostatic Sprayer for Four-Wheel Independent Drive/Steering Facility. Master's Thesis, Shandong Agricultural University, Taian, China, 2022.
24. Zhang, R. Design and Experimental Study of Control System of Target Variable Spray Device in Greenhouse. Master's Thesis, Jiangsu University, Zhenjiang, China, 2022.
25. Yang, Z.; Yu, C.; Yang, H.; Chen, Y.; Zhou, X.; Ma, Y.; Wang, X. Design and test of greenhouse target spray robot based on LiDAR. *J. Agric. Mech. Res.* **2022**, *44*, 83–89.
26. Zhang, Y. *Design and Test of Integrated Air-Fed Electrostatic Fogging System in Solar Greenhouse*; Shandong Agricultural University: Taian, China, 2022.
27. *JB/T 9782-2014*; General Test Methods for Plant Protection Machinery. China Quality Inspection Press: Beijing, China, 2014.